Sustainable Method for Alzheimer Dementia Prediction in Mild Cognitive Impairment: Electroencephalographic Connectivity and Graph Theory Combined with Apolipoprotein E

Dr Fabrizio Vecchio, PhD,[1] Dr Francesca Miraglia, PhD,[1,2] Dr Francesco Iberite,[1] Dr Giordano Lacidogna,[3] Dr Valeria Guglielmi,[3] Dr Camillo Marra,[2,3] Dr Patrizio Pasqualetti,[4] Dr Francesco Danilo Tiziano,[5] and Prof Paolo Maria Rossini[2,6]

Objective: Mild cognitive impairment (MCI) is a condition intermediate between physiological brain aging and dementia. Amnesic-MCI (aMCI) subjects progress to dementia (typically to Alzheimer-Dementia = AD) at an annual rate which is 20 times higher than that of cognitively intact elderly. The present study aims to investigate whether EEG network Small World properties (SW) combined with Apo-E genotyping, could reliably discriminate aMCI subjects who will convert to AD after approximately a year.
Methods: 145 aMCI subjects were divided into two sub-groups and, according to the clinical follow-up, were classified as Converted to AD (C-MCI, 71) or Stable (S-MCI, 74).
Results: Results showed significant differences in SW in delta, alpha1, alpha2, beta2, gamma bands, with C-MCI in the baseline similar to AD. Receiver Operating Characteristic(ROC) curve, based on a first-order polynomial regression of SW, showed 57% sensitivity, 66% specificity and 61% accuracy(area under the curve: AUC=0.64). In 97 out of 145 MCI, Apo-E allele testing was also available. Combining this genetic risk factor with Small Word EEG, results showed: 96.7% sensitivity, 86% specificity and 91.7% accuracy(AUC=0.97). Moreover, using only the Small World values in these 97 subjects, the ROC showed an AUC of 0.63; the resulting classifier presented 50% sensitivity, 69% specificity and 59.6% accuracy. When different types of EEG analysis (power density spectrum) were tested, the accuracy levels were lower (68.86%).
Interpretation: Concluding, this innovative EEG analysis, in combination with a genetic test (both low-cost and widely available), could evaluate on an individual basis with great precision the risk of MCI progression. This evaluation could then be used to screen large populations and quickly identify aMCI in a prodromal stage of dementia.

ANN NEUROL 2018;84:302–314

Mild cognitive impairment (MCI) is a clinical and neuropsychological state in the elderly brain that is intermediate between normal cognition and dementia. It is mainly characterized by objective evidence of memory impairment during a neuropsychological examination that does not yet encompass the definition of dementia.[1,2] Epidemiological research suggests that amnesic MCI (aMCI) is a precursor to Alzheimer dementia

View this article online at wileyonlinelibrary.com. DOI: 10.1002/ana.25289

Received Apr 20, 2017, and in revised form Jul 3, 2018. Accepted for publication Jul 3, 2018.

Address correspondence to Dr Rossini, Institute of Neurology, Area of Neuroscience, Catholic University, Policlinic A. Gemelli Foundation, Rome, Italy. E-mail: paolomaria.rossini@policlinicogemelli.it

From the [1]Brain Connectivity Laboratory, IRCCS San Raffaele Pisana; [2]Institute of Neurology, Area of Neuroscience, Catholic University of The Sacred Heart; [3]Neuropsychological Center, Catholic University of The Sacred Heart; [4]Service of Medical Statistics and Information Technology, Fatebenefratelli Foundation for Health Research and Education, AFaR Division; [5]Institute of Medical Genetics, Catholic University, Policlinic A. Gemelli Foundation; and [6]Fondazione Policlinico Universitario A.Gemelli IRCCS, Rome, Italy

(AD),[3] based on the high rate of progression from this state to AD.[2] About 50% of all MCI subjects convert to dementia.[4–7] The others will either remain in the MCI condition or return to a fully normal one and never progress to dementia.

To plan optimal and early therapeutic, organizational, lifestyle, and rehabilitative interventions, aMCI diagnosis should be combined with the most reliable prognosis on the likelihood and time of progression to dementia. Growing evidence suggests that early diagnosis reduces the health and social costs associated with dementia management.[8,9] Moreover, prodromal MCI to AD is becoming the preferred target for clinical trials with potentially disease-modifying experimental drugs. Because such a high risk is associated with the MCI condition, it is important to increase the success rate of the trials conducted. The early diagnosis of prodromal MCI to AD can presently be reached with a high degree of sensitivity and specificity by combining a number of tests (eg, hippocampal volumetric magnetic resonance imaging [MRI], positron emission tomography [PET], or PET integrated with beta-amyloid and tau radioligands and lumbar puncture for cerebrospinal fluid beta and tau metabolites). Due to their high costs, limited availability, and/or body invasiveness, however, these tests cannot be used to screen a large population sample.

Electroencephalogram (EEG) is an ideal candidate for such screening, because it is a widely available, noninvasive, and low-cost[10] procedure. Moreover, a great deal of research has been conducted on EEG abnormalities in pathological brain aging.[11] AD patients show more delta and fewer posterior alpha EEG rhythms than cognitively intact elderly (Nold) subjects.[12] Similarly, MCI show less alpha power than Nold subjects.[13] Furthermore, a reduction in EEG spectral coherence in the alpha band in AD has been reported,[14,15] and EEG theta power was found to be higher in aMCI subjects who will convert to AD. High predictive accuracy between baseline EEG features and the probability of a future decline was found.[16] Furthermore, EEG coherence has been shown to contribute to the differentiation of AD from Nold[15] and to the prediction of aMCI conversion to AD.[14] However, findings were usually significant only at a group level[17]; moreover, relatively small samples were investigated, with a briefer than required follow-up. Despite such limitations, the progression of the diagnosis of AD has been summarized in a review,[18] showing generalized slowing of the rhythms contained in the spectral profile, reduced complexity, and perturbations in EEG organization. Furthermore, the corticocortical connectivity and network properties of EEG have been addressed in several studies.[11,19–21] Many of the studies have also explored the idea that dementias—particularly in the very early, namely prodromal, stages—mainly affect synaptic transmission and therefore represent "disconnection syndromes."[22]

Network science tends to model the brain as an intricate amalgamation of networks; a network is a mathematical representation of a real-world complex system, which is defined by a collection of nodes (vertices) and links (edges) between pairs of nodes. Nodes usually represent brain regions, whereas links represent anatomical, functional, or effective connections, depending on the dataset.[23] Anatomical connections typically correspond to white matter fiber tracts between pairs of gray matter brain regions (cortical areas or subcortical relays). Connections between neuronal assemblies reflect segregation and integration processes, as revealed by local clustering (segregation) and path length (integration). Brain connections are organized in a network topology characterized by a high degree of local clustering (segregation) and long-distance connections (integration). A "small world" (SW) concept was introduced as a model of network organization, allowing for an optimal balance between local specialization and global integration.[24] This approach could be used to model brain functional architecture[25] and correlate it with behavior (ie, neuropsychological test performance). This evaluates whether functional connectivity patterns between brain areas reproduce the organization of more or less strictly bound networks based on the strength of oscillatory firing synchronizations between adjacent/remote neuronal assemblies in a time frame of milliseconds.[26–30] In recent literature, several studies have utilized graph theory analysis of connectivity from EEG signals combined with apolipoprotein E (ApoE) genotyping to discriminate between healthy elderly and AD patients.[31,32] No previous studies utilized such an approach to distinguish prodromal to AD from nonprodromal MCI subjects.

The primary aim of the present study was to investigate brain connectivity using a SW approach for the analysis of EEG-related neural networks. Moreover, as the ε4 allele of the *APOE* gene is a genetically determined risk factor for the pathogenesis of late onset and sporadic AD, a secondary endpoint is to investigate whether EEG connectivity markers along with genetically determined risk indicators for dementia, as represented by ApoE testing, can reach a greater sensitivity/specificity for the stage of MCI prodromal to AD.[33,34] Our purpose is to provide a reliable, low-cost, widely available, and noninvasive method for discrimination of high-risk aMCI subjects, namely those who, on an individual basis, will rapidly (ie, after 1 or 2 years) convert to AD.

Patients and Methods

Participants

The ages of the 145 aMCI subjects at the time of the EEG recordings were 71.83 ± 0.56 standard error of the mean (SEM) years, Mini-Mental State Examination (MMSE) was 25.87 ± 0.18, and gender distribution was 82 females (F) and 63 males (M). The participants, all of whom were affected by aMCI, had been referred to the Memory Clinic of the Catholic University, Policlinic A. Gemelli Foundation in Rome.[4,35,36] They were divided into 2 subgroups according to their clinical evolution, classified as converted to AD or stable aMCI (aMCI-S) after a follow-up from time 0 (diagnosis of MCI). At the end of the follow-up, it was shown that at the time of the EEG recordings, the patient group included 74 aMCI-S (age = 70.72 ± 0.77 SEM years, MMSE = 26.33 ± 0.27, months of follow-up = 38.17 ± 3.48, M/F = 33/41) and 71 converted aMCI (aMCI-C; age = 73.05 ± 0.81 SEM years, MMSE = 25.32 ± 0.23, months of follow-up = 18.29 ± 1.60, M/F = 35/36). The time interval between aMCI diagnosis and EEG recording was <1 month in both groups and at an individual level. As an EEG control group, 175 AD age-matched patients were selected (age = 72.23 ± 0.55 years, MMSE = 20.12 ± 0.31 years, M/F = 81/94).

All subjects were right-handed, according to the Handedness Questionnaire. Individual informed consent was obtained, and the study was approved by a local ethics committee. Experimental procedures conformed to the Declaration of Helsinki and national guidelines.

Inclusion and Exclusion Criteria

All subjects took part in a battery of neuropsychological tests assessing attention, memory, executive functions, visuoconstruction abilities, and language. Memory was assessed via the immediate and delayed recall of the Rey Auditory Verbal Learning Test, the delayed recall of Rey figures, the delayed recall of a 3-word list, and the delayed recall of a story. An MCI amnesic diagnosis hinged upon an impairment in an at least 1 episodic memory test. The abnormal threshold for performances on the memory tasks was set below the 5th percentile of the healthy population. The exclusion criteria included traumatic head injuries, epilepsy, alcoholism, and the occurrence of any other past neurological or psychiatric diseases. The patients were carefully screened for medical conditions that could potentially be associated with cognitive disturbances (ie, renal or hepatic failure, thyroid dysfunction, and folate and/or vitamin B12 deficits).

Each subject also underwent brain MRI and single photon emission computed tomography (SPECT), MMSE, Clinical Dementia Rating, and an assessment of their Geriatric Depression Scale (GDS), Hachinski Ischemic Score, and Instrumental Activities of Daily Living scale to confirm the diagnosis and to exclude other causes of dementia, such as frontotemporal dementia, vascular dementia, extrapyramidal syndromes, reversible dementias, and Lewy body dementia. This was performed to ensure the creation of clinically homogeneous groups.

AD was diagnosed according to the National Institute on Aging–Alzheimer's Association workgroups[36] and the Diagnostic and Statistical Manual of Mental Disorders, 4th edition, text revision criteria. Moreover, the affected individuals showed a significant reduction in hippocampal volume and an increase in the width of the temporal horn and choroidal fissure (ranging between 2 and 4 on the Likert scale). The pattern of blood flow and oxygen consumption on SPECT was abnormal as well.

The exclusion criteria for AD focused upon any evidence of (1) frontotemporal dementia, (2) behavioral variants of frontotemporal dementia, (3) vascular dementia, (4) extrapyramidal syndromes, (5) reversible dementias (including pseudodementia of depression), and (6) Lewy body dementia.

aMCI was diagnosed according to guidelines and clinical standards.[2,37,38] The exclusion criteria for aMCI were: (1) mild AD, as diagnosed by standard protocols, including the National Institute on Aging–Alzheimer's Association workgroups[36]; (2) clinicoinstrumental evidence of concomitant dementia, such as frontotemporal, vascular, and reversible dementias (including pseudodepressive dementia), marked fluctuations in cognitive performance compatible with Lewy body dementia and/or features of mixed dementias; (3) evidence of concomitant extrapyramidal symptoms; (4) clinical and indirect evidence of depression, as revealed by the GDS (scores < 14 [no depression]); (5) other psychiatric diseases, including epilepsy, drug addiction, alcohol dependence, or the use of neuro-/psychoactive drugs (including acetylcholinesterase inhibitors); and (6) current or previously uncontrolled or complicated systemic diseases (including diabetes mellitus) or traumatic brain injuries.

Follow-up visits, including neuropsychological tests, were carried out every 6 months to intercept the epoch of an eventual MCI-to-AD conversion.

Data Recordings and Preprocessing

The EEG recording was performed at rest, on individuals with closed eyes and in no-task conditions (for at least 5 minutes). The subjects were seated and relaxed in a sound-attenuated and dimly lit room. EEG signals were recorded with a standard montage from 19 electrodes (Fp1, Fp2, F7, F8, F3, F4, T3, T4, C3, C4, T5, T6, P3, P4, O1, O2, Fz, Cz, and Pz) positioned on the scalp,

according to the international 10-20 system. Eye movements were monitored from 2 different channels with vertical and horizontal montages. Skin/electrode impedances were lowered to <5kΩ.

Data were analyzed with MATLAB R2011b software (MathWorks, Natick, MA) using scripts from the EEGLAB 11.0.5.4b toolbox (Swartz Center for Computational Neurosciences, La Jolla, CA; sccn.ucsd.edu/eeglab). The EEG recordings were band-pass filtered from 0.2 to 47Hz using a finite impulse response filter and a 256Hz sampling rate. Ocular, muscular, cardiac, and other types of artifacts were inspected on imported data fragmented in 2-second duration epochs. The procedure was as follows: (1) the data were reviewed, and the epochs with aberrant waveforms or with evident artifactual activity were manually discarded by an expert in EEG; and (2) the detection and rejection of artifacts were completed through an independent component analysis (ICA) using the Infomax ICA algorithm, as implemented in EEGLAB. ICA is a blind source decomposition algorithm that enables the separation of statistically independent sources from multichannel data. It is considered an effective method for separating ocular movements and blink artifacts from EEG data. The components were visually inspected, and if artifact contamination was found, they were manually rejected by the investigator.

Functional Connectivity Analysis

EEG functional connectivity analysis was performed using low-resolution brain electromagnetic tomography (eLORETA) exact low-resolution electromagnetic tomography software.[26,27,39,40] The eLORETA algorithm is a linear inverse solution for EEG signals with no localization error that can indicate sources under ideal (noise-free) conditions.[41] According to the scalp-recorded EEG potential distribution, eLORETA software was used to compute a discrete, 3-dimensionally distributed linear, weighted, minimum-norm inverse solution. The particular weights used in eLORETA endow the tomography with the property of exact localization necessary to test point sources, yielding images of the current density with exact localization, albeit with a low spatial resolution (ie, the neighboring neuronal sources are highly correlated).

To obtain a topographic view of the whole brain, brain connectivity was computed with eLORETA software in 84 regions, positioning the center in the 42 available Brodmann areas (BAs; 1, 2, 3, 4, 5, 6, 7, 8, 9, 10, 11, 13, 17, 18, 19, 20, 21, 22, 23, 24, 25, 27, 28, 29, 30, 31, 32, 33, 34, 35, 36, 37, 38, 39, 40, 41, 42, 43, 44, 45, 46, and 47) in the left and right hemispheres.

Regions of interest (ROIs) are needed for estimation of the electric neuronal activity that is used to analyze brain functional connectivity. The signal at each cortical ROI consisted of the average electric neuronal activities of all voxels belonging to that ROI, as computed with eLORETA. For each hemisphere, among the eLORETA current density time series of the 84 ROIs, the intracortical lagged linear coherence, extracted via the "all nearest voxels" method,[42] was computed between all possible pairs of the 84 ROIs for each of the 7 independent EEG frequency bands of delta (2–4Hz), theta (4–8Hz), alpha 1 (8–10.5Hz), alpha 2 (10.5–13Hz), beta 1 (13–20Hz), beta 2 (20–30Hz), and gamma (30–45Hz) for each subject.

Starting with the definition of the complex valued coherence between time series x and y in the frequency band ω—which is based on the cross-spectrum given by the covariance and variance of the signals—the lagged linear coherence in the frequency band ω is reported in accordance with the following equation,[42]

$$LagR^2_{xyw} = \frac{[ImCov(x,y)]^2}{Var(x)*Var(y) - [ReCov(x,y)]^2}$$

where *Var* and *Cov* are the variance and covariance of the signals.

This was developed as a measure of true physiological connectivity not affected by volume conduction and low spatial resolution.[42] The values of lagged linear connectivity computing between all pairs of ROIs for each frequency band were used as weights of the networks built in the graph analysis.

Graph Analysis

As previously stated, a network is a mathematical representation of a real-world complex system. It is defined by a collection of nodes (vertices) and links (edges) between pairs of nodes. Nodes usually represent brain regions, whereas links represent anatomical, functional, or effective connections,[23] depending on the dataset. Anatomical connections typically correspond to white matter fiber tracts between pairs of gray matter brain regions (cortical areas or subcortical relays). Functional connections correspond to magnitudes of temporal correlations in activity and may occur between pairs of anatomically unconnected regions.

A weighted graph is a mathematical representation of a set of elements (vertices) that may be linked through connections of variable weights (edges).

In the present study, the weighted and undirected networks were built (the vertices of the network were the estimated cortical sources in the BAs) and the edges were weighted by the lagged linear value within each pair of vertices. The software instrument used here for the graph

analysis was the Brain Connectivity Toolbox (http://www.brain-connectivity-toolbox.net/), adapted with our own MATLAB scripts.

The SW parameter was evaluated on the brain networks, as it measures the balance between local connectedness and the global integration of a network, representing brain network organization. SW architecture is intermediate between that of random networks (associated with a short overall path length but a low level of local clustering) and regular networks or lattices (which have a high level of clustering but a high overall path length); specifically, SW networks have a relatively high level of clustering and a short path length.[43] The measure of network small-worldness was defined as the ratio of the normalized clustering coefficient (Cw) and the normalized path length (Lw). We used data normalization (ie, relativization) before performing the SW measurements. The normalized characteristic path length was obtained dividing the parameter by a mean value. The mean value is the average of the characteristic path length values of each subject within the 7 EEG frequency bands. The same procedure was applied to compute the normalized clustering coefficient. As we computed from weighted networks, it was difficult to evaluate disgraphs with the same number of nodes and connections (all connections were available), so we decided to use relative values within bands.[11,19–21]

ApoE Testing

In a subgroup of 97 subjects (age = 71.46 ± 0.66 SEM years, MMSE = 25.98 ± 0.22)—52 aMCI-S (age = 69.85 ± 0.89 years, MMSE = 26.74 ± 0.29, months of follow-up = 45.87 ± 3.94, M/F = 22/30) and 45 aMCI-C (age = 73.33 ± 0.92 years, MMSE = 25.11 ± 0.27, months of follow-up = 19.75 ± 1.82, M/F = 19/26)—blood genotyping was performed. The ApoE genotype was determined following the well-established method pioneered by Hixson and Vernier.[44] During a further classification process, we considered the MCI subjects to be ApoE4 noncarriers (absence of the ε4 allele) or ApoE4 carriers (presence of at least 1 ε4 allele).

Statistical Evaluation

The eLORETA statistical evaluation was performed using a graph analysis pattern extracted with sLORETA/eLORETA from the brain network. The normality of the data was tested using the Kolmogorov–Smirnov test, and the hypothesis of Gaussianity could not be rejected. To confirm the working hypothesis, a statistical analysis of variance (ANOVA) design was addressed for the SW between the factors Group (aMCI-C, aMCI-S) and Band (delta, theta, alpha 1, alpha 2, beta 1, beta 2, and gamma). An ANOVA design was also incorporated for the SW between the factors Group (AD, aMCI-C, aMCI-S) and Band (delta, theta, alpha 1, alpha 2, beta 1, beta 2, gamma).

Polynomial Regression and Receiver Operating Characteristic Curve and 10-Fold Cross-Validation

The dataset contains the SW value of the brain network for the 145 subjects at the 7 given EEG frequency bands: delta, theta, alpha 1, alpha 2, beta 1, beta 2, and gamma. Each subject has been assigned a label according to whether he or she developed AD at the follow-up.

A simple polynomial regression has been chosen, calculated using the MATLAB built-in function "fitlm"; the function fits, using the least squares method, a given polynomial. The polynomial contains 8 coefficients: the constant term and a coefficient for each of the frequency bands. The residuals plot showed an almost normal distribution, suggesting that an appropriate polynomial was chosen for the approximation.

The data were randomly distributed across the 10 groups in accordance with the 10-fold cross-validation technique, and the classifier was tested against all of the groups while being trained on the other 9. The resulting performances and areas under the receiver operating characteristic (ROC) curve (AUC) were averaged to compute the final value.

The following indexes measured the performance of the conversion binary classification: (1) sensitivity, which measures the rate of the positives (aMCI-C) who were correctly classified as positives (ie, they were assigned a "true positive rate" using the signal detection theory); (2) specificity, which measures the rate of the negatives (aMCI-S) who were correctly classified as negatives (ie, they were assigned a "true negative rate" using the signal detection theory); (3) accuracy of the classifier (subjects correctly classified); and (4) AUC. We reported sensitivity, specificity, and accuracy only for the "optimal" values (with the cutoff point corresponding to the maximal accuracy).

Finally, we included ApoE genotyping in the dataset. The dataset contained the same SW value of the brain network for the 97 subjects at the 7 given EEG frequency bands: delta, theta, alpha 1, alpha 2, beta 1, beta 2, and gamma. Added to the code of *APOE*-ε4 noncarrier or *APOE*-ε4 carrier was a polynomial containing 9 coefficients: the constant term, the ApoE, and a coefficient for each of the frequency bands. Each subject was assigned a label corresponding to the outcome (ie, whether the individual had converted to AD at the follow-up).

Results

Clinical Data

The clinical and demographic data of the whole group of subjects are reported in Table 1, showing that the 2 groups present no differences.

Graph Theory Parameter Analysis

ANOVAs for the evaluation of both Cw and Lw showed statistically significant interactions (Cw: $F_{6,\ 858} = 3.7042$, $p = 0.00122$; Lw: $F_{6,\ 858} = 4.1535$, $p < 0.0004$) between the Group (aMCI-C, aMCI-S) and EEG Band (delta, theta, alpha 1, alpha 2, beta 1, beta 2, gamma) factors. Duncan-planned post hoc testing showed higher values in both coefficients in the delta ($p < 0.04$) band, and lower values in alpha 1 ($p < 0.004$) and alpha 2 bands ($p < 0.011$) in aMCI-C, with respect to the aMCI-S subjects.

The ANOVA for the evaluation of the SW showed a statistically significant interaction ($F_{6,\ 858} = 7.6633$, $p < 0.00001$) between the Group (aMCI-C, aMCI-S) and EEG Band (delta, theta, alpha 1, alpha 2, beta 1, beta 2, gamma) factors. Duncan-planned post hoc testing showed lower values of SW coefficients in the delta ($p < 0.034$), beta 2 ($p < 0.032$), and gamma ($p < 0.0001$) bands and vice versa for the higher SW in the alpha 1 ($p < 0.011$) and alpha 2 frequency bands ($p < 0.0005$) in aMCI-C, with respect to the aMCI-S subjects.

To evaluate eventual differences in the AD condition, this second analysis was performed. For the evaluation of SW between the factors Group (AD, aMCI-C, aMCI-S) and Band (delta, theta, alpha 1, alpha 2, beta 1, beta 2, gamma), ANOVA showed a statistical interaction ($F_{12,\ 1,914} = 7.5748$, $p < 0.00001$), as plotted in Figure 1. Duncan-planned post hoc testing showed no statistical differences between AD and aMCI-C subjects, except in the gamma band ($p < 0.00002$).

Figure 2 reports the functional coupling distribution, as revealed by the lagged linear coherence, in all EEG frequency bands in the 2 subgroups of aMCI subjects. It is evident, as has already been illustrated in several previous studies (including one of ours), that aMCI-C presents greater coupling in delta and lower in alpha than aMCI-S.

ApoE Testing

Among the 97 subjects with the ApoE classification, of the 66 ApoE4 noncarriers (lacking the ε4 allele), 29 converted (43.9%). Meanwhile, among the 31 ApoE4 carriers (with at least 1 ε4 allele), 16 (51.6%) converted. The ROC (red line in Fig 3) curve showed an AUC of 0.51.

TABLE 1. Clinical Data of the 2 Groups of Amnesic Mild Cognitive Impairment

	Stable		Converted	
	Mean	SE	Mean	SE
Educational level	10.15	0.71	10.02	0.70
RAVLT immediate recall	26.95	1.19	24.50	0.99
RAVLT delayed recall	3.87	0.49	2.32	0.34
RAVLT recognition correct	10.34	0.53	9.06	0.72
RAVLT recognition false	4.97	0.97	4.31	1.00
RAVLT recognition accuracy	0.85	0.02	0.81	0.03
Constructional praxis	9.26	0.36	8.59	0.41
Constructional praxis landmarks	66.26	0.75	64.85	1.03
MFTC accuracy	0.96	0.01	0.90	0.02
MFTC false alarms	0.43	0.18	1.55	0.65
MFTC time	95.96	5.04	96.52	9.29
Raven Matrices ′47	24.53	0.99	25.13	2.84
Phonological verbal fluency	30.57	1.94	25.09	1.38
Categorical verbal fluency	10.96	0.83	10.52	0.65
Stroop SF interference time	33.71	3.93	55.52	9.19
Stroop SF Interference errors	1.89	0.58	5.19	1.56
Corsi forward	4.69	0.26	3.71	0.39
Corsi backward	3.50	0.29	3.60	0.24
Clock-drawing	3.13	0.44	2.43	0.53
Prose memory	3.63	1.08	1.43	0.57
Span forward	5.23	0.30	5.22	0.32
Span backward	4.00	0.41	3.17	0.40

MFTC = Multiple Features Target Cancellation; RAVLT = Rey Auditory Verbal Learning Test; SE = standard error; SF = short form.

Classification between Stable and Converted Individuals Based on SW

In the classification process considering only the SW values (145 subjects), the ROC (green line in Fig 3) curve

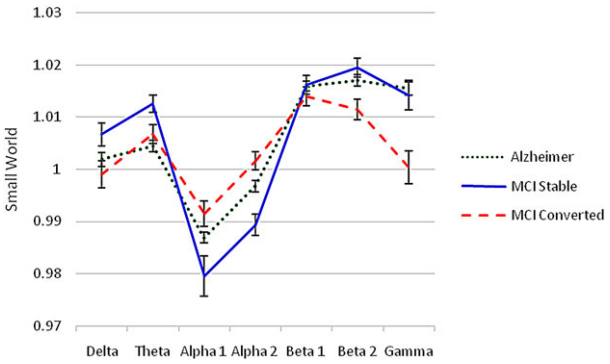

FIGURE 1: Small world characteristics across electroencephalographic frequency bands in stable and converted amnesic mild cognitive impairment (MCI) subjects with respect to Alzheimer dementia patients.

showed an AUC of 0.64 (indicating moderate classification accuracy). The resulting classifier showed 57% sensitivity, 66% specificity, and 61% accuracy for the classification of the aMCI state as a prodromal indicator of AD. This result was obtained when all subjects were included.

When adding ApoE genotyping to the classification process (using 97 subjects), the ROC curve (blue line in Fig 3) showed an AUC of 0.97; the resulting classifier presented 96.7% sensitivity, 86% specificity, and 91.7% accuracy, indicating very high accuracy for the classification of the aMCI state as prodromal to AD. Using only the SW values in these 97 subjects, the ROC curve showed an AUC of 0.63; the resulting classifier presented 50% sensitivity, 69% specificity, and 59.6% accuracy.

Of note, it is possible to consider the point density in the ROC curve as a measure of stability to threshold changes; in that regard, it is clear that the most stable (although not the highest performing) classifier is the one that relies only on ApoE, as it evaluates only one variable with 1 and 0 as possible values. Comparing SW to SW + ApoE, it is possible to state that, by adding genotype information, classification performance increases and stability improves.

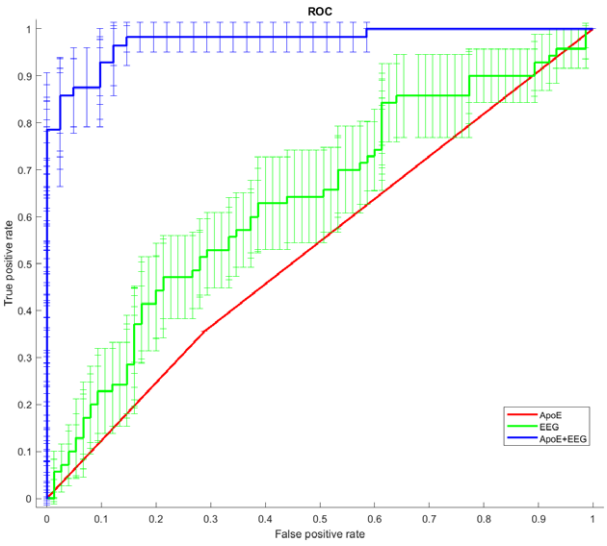

FIGURE 3: Average receiver operating characteristic (ROC) curves and their confidence intervals, illustrating the classification of the stable and converted amnesic mild cognitive impairment individuals based on the apolipoprotein E (ApoE; red line, 97 patients), small world (green line, 145 patients), and ApoE + electroencephalographic (EEG; blue line, 97 patients) values. The area under the ROC curves was, respectively, 0.52, 0.64, and 0.97, indicating an optimal classification accuracy.

Control Analyses

Figure 4 illustrates the connection matrices related to the 2 groups aMCI-C and aMCI-S (indicating the baseline functional network topology).

To understand whether the difference in the baseline could influence the results, we selected 2 subgroups that were perfectly homogeneous in terms of their demographic and cognitive parameters. The subgroups included

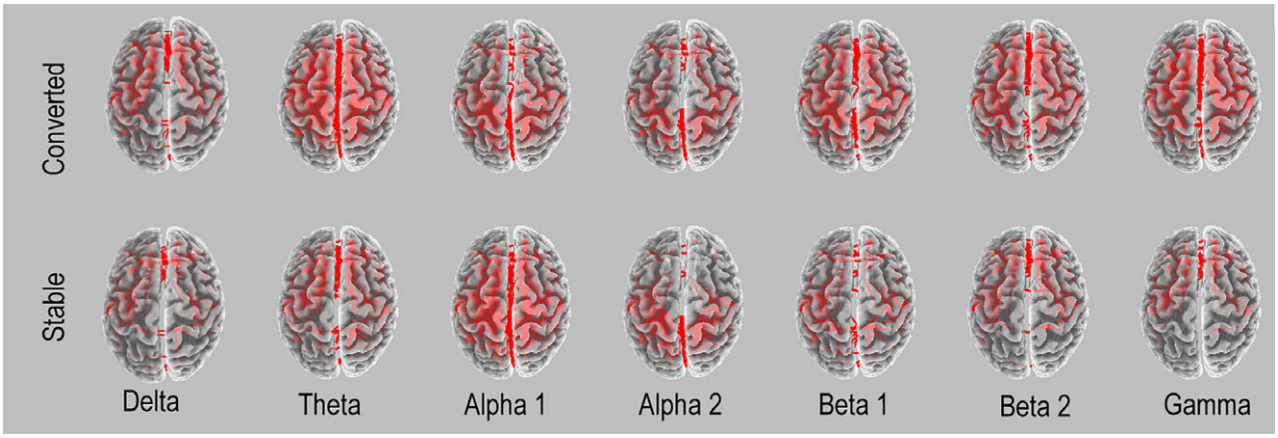

FIGURE 2: Functional coupling in stable and converted subjects. An arbitrary threshold was used to illustrate these patterns. It is evident that converted amnesic mild cognitive impairment presented more coupling in delta and beta and gamma, and less coupling in alpha than stable mild cognitive impairment.

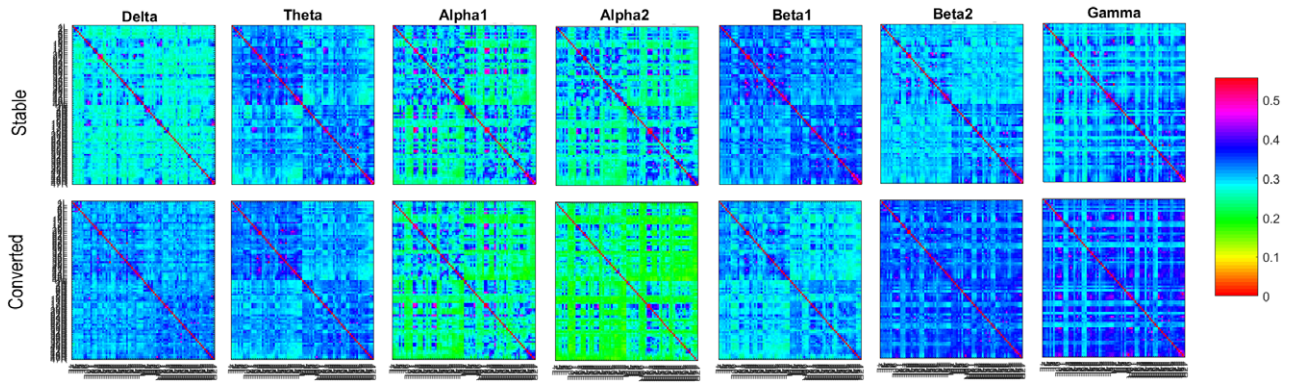

FIGURE 4: Square image representation lagged linear coherence of each band both before and after. In the axes, there are reported the single nodes of the network: Brodmann areas 1F, 2P, 3F, 4F, 5P, 6F, 7P, 8F, 9F, 10F, 11F, 13F, 17O, 18O, 19O, 20T, 21T, 22T, 23P, 24F, 25F, 27T, 28T, 29T, 30T, 31P, 32F, 33F, 34T, 35T, 36T, 37T, 38T, 39P, 40P, 41T, 42T, 43P, 44F, 45F, 46F, and 47F first in the left and then in the right hemisphere, where F, T, O and P represent frontal, temporal, occipital, and parietal, respectively.

42 aMCI-S and 43 aMCI-C subjects. Furthermore, 27 aMCI-S and 30 aMCI-C subjects also presented ApoE testing values (demographic data are reported in Table 2). For these groups, we performed the same classifier procedures as in the main analyses of the present study. Our results were in line with the main results, but were not as statistically significant, probably because of the small number of patients, who showed an AUC of 0.62. The resulting classifier showed 52% sensitivity, 90% specificity, and 61% accuracy. When adding ApoE genotyping to the classification process, the ROC curve showed an AUC of 0.7; the resulting classifier presented 67% sensitivity, 93% specificity, and 65% accuracy.

Is the need for a "graph theoretical" model supported by the present results? To answer this question, we compared the same type of classifier to other methods of EEG analysis currently used for AD studies and applied what was found to the same EEG epochs utilized for graph valuation, namely spectral coherence and power spectrum in combination with ApoE. Our most significant result was obtained when analyzing the power density spectrum on all available subjects. We used sLORETA software to solve the EEG inverse problem within a 3-shell spherical head model and to find the values of the voxel current density, to explain the EEG spectral power density recorded by the scalp electrodes. The current density at each voxel was then normalized to the power density averaged across all the frequencies (0.5–45Hz) and across all 6,239 voxels of brain volume. After this normalization, the current density values lost their original physical dimension and were represented by an arbitrary unit scale. This procedure also reduced intersubject variability.

In line with the low spatial resolution of the adopted technique, we used ROI marker sLORETA software to collapse the voxels of sLORETA solutions at 12 ROIs (6 for the left and 6 for the right hemispheres; BAs included in the cortical regions of interest: frontal [8, 9, 10, 11, 44, 45, 46, 47], central [1, 2, 3, 4, 6], parietal [5, 7, 30, 39, 40, 43], occipital [17, 18, 19], temporal [20, 21, 22, 37, 38, 41, 42], and limbic [31, 32, 33, 34, 35, 36]) coded according to the Talairach space. The signal at each cortical ROI consists of the averaged electric neuronal activities of all voxels belonging to that ROI, as computed with sLORETA. The current densities at different voxels were then grouped to describe the cerebral activity in the following EEG frequency bands: delta (2–4Hz), theta (4–8Hz), low alpha (8–10.5Hz), high alpha (10.5–13Hz), low beta (13–20Hz), high beta (20–30Hz), and gamma (30–45Hz). The sLORETA method is a properly standardized, discrete, linear, minimum-norm, inverse-solution method that computes the 3-dimensional cortical distribution of the electric neuronal source activity from the EEG recordings on the head surface.[45] A detailed description of the method can be found in several previous publications.[41]

In accordance with the data, we performed the classifier procedures of the main analyses of the present study and obtained 51.79% sensitivity, 100% specificity, and 68.86% accuracy; these results are promising but show less significance than those in our proposal.

Discussion

AD is characterized by a progressive loss of memory and deterioration of other cognitive functions. The illness has a prolonged and progressive course, and patients—if they survive long enough to experience the late form of the disease—die in a nearly vegetative state. The disease characteristics place an enormous emotional and financial burden on patients, their families, and society.[46] In 2010,

TABLE 2. Clinical Data of the 2 Homogeneous Subgroups of Amnesic Mild Cognitive Impairment

	42 Stable		43 Converted		27 Stable		30 Converted	
	Mean	SE	Mean	SE	Mean	SE	Mean	SE
MMSE	26.09	0.34	25.63	0.27	26.60	0.39	25.47	0.36
Age	71.71	0.89	72.02	1.05	71.15	1.00	72.27	1.12
Education level	9.36	0.75	10.07	0.79	9.56	0.91	9.83	0.93
RAVLT immediate recall	25.91	1.23	25.38	1.07	26.24	1.56	25.90	1.42
RAVLT delayed recall	2.97	0.43	2.61	0.44	3.05	0.55	2.92	0.56
RAVLT recognition correct	10.41	0.58	9.73	0.70	9.76	0.81	9.65	1.03
RAVLT recognition false	5.36	1.02	5.35	1.24	5.25	0.93	6.24	1.76
RAVLT recognition accuracy	0.82	0.02	0.83	0.02	0.83	0.02	0.82	0.03
Constructional praxis	9.16	0.28	9.00	0.38	8.87	0.35	8.08	0.35
Constructional praxis landmarks	66.00	0.60	64.55	1.10	65.93	0.82	62.54	1.48
MFTC accuracy	0.97	0.01	0.91	0.02	0.97	0.01	0.90	0.03
MFTC false alarms	1.24	0.72	1.25	0.47	1.44	1.01	1.35	0.58
MFTC time	79.38	5.61	81.64	6.13	83.19	7.14	82.07	8.47
Raven Matrices ′47	24.88	1.02	22.44	1.06	25.10	1.35	21.98	1.33
Phonological verbal fluency	29.00	1.55	28.13	1.44	27.80	1.92	28.56	2.00
Categorical verbal fluency	13.30	0.71	10.87	0.74	12.94	0.90	11.69	0.94
Stroop SF interference time	41.54	5.99	42.50	6.86	36.55	5.18	37.54	5.00
Stroop SF interference errors	2.18	0.54	2.55	0.56	3.10	0.56	3.13	0.76
Corsi forward	4.70	0.19	4.25	0.17	5.50	0.47	4.67	0.13
Corsi backward	3.50	0.13	3.33	0.11	3.50	0.16	3.33	0.13
Clock-drawing	3.13	0.23	3.17	0.18	3.14	0.30	3.20	0.24
Span forward	5.20	0.21	5.00	0.23	5.00	0.32	5.00	0.32
Span backward	4.00	0.26	3.50	0.18	3.50	0.47	3.50	0.22

Subjects with apolipoprotein E are shown on the right.

MFTC = Multiple Features Target Cancellation; MMSE = Mini-Mental State Examination; RAVLT = Rey Auditory Verbal Learning Test; SE = standard error; SF = short form.

AD cost the United States an estimated $604 billion. This number is staggering, especially in light of predictions that the number of AD cases worldwide, currently estimated at 36 million, will triple by 2050.[9] The US costs of dementia were estimated to total $818 billion in 2015, an increase of 35% since 2010; 86% of the expenses are incurred in high-income countries. The costs of informal care and the direct costs of social care represent similar proportions of the total cost, whereas the costs incurred by the medical sector are much lower. A threshold of US $1 trillion was predicted to be crossed by 2018.[47]

The AD clinical phenotype follows a prodromal stage known as MCI, which is usually characterized by memory loss (aMCI). The identification of early biomarkers of conversion from aMCI to AD are of interest to researchers and health policy makers when the goal of early interventions is pursued. Even in the absence (at the present) of a disease-modifying therapy, it is evident that the early initiation of pharmacological and nonpharmacological treatments (including changes in lifestyle) helps to maintain personal autonomy in daily activities and significantly reduces the total costs of disease management.[48–50]

Moreover, many of the clinical trials with potentially disease-modifying drugs target MCI subjects who are prodromal to AD, because failure has been demonstrated when the full symptomatology of AD has already been developed. Therefore, biomarkers that can carefully predict the evolution of the disease at an early stage could be instrumental in enabling early diagnosis and intervention and could be used to identify individuals who could benefit from trials with experimental drugs. This can be partly accomplished with the presently available diagnostic armamentarium (volumetric MRI, PET, PET + radioligands/lumbar puncture for amyloid and tau metabolites), although it has a relatively low sensitivity to synaptic dysfunction (which is associated with a very early stage of presymptomatic AD) and is definitely expensive, limited in terms of its availability on a territorial level, and relatively invasive. Because of these limitations, such a diagnostic combination is not feasible for a large population screening. A recent survey and meta-analysis yielded a prevalence of the MCI condition of 5.9% in the > 60-year-old population, with a steady progression in the different age groups (4.5% 60–69, 5.8% 70–79, 7.1% 80–89; Cohort Studies Memory in an International Consortium).[51] These represent significant numbers for a population-based screening. In recent years, progressively more attention has been paid to the electrophysiological substrate of the disease, which could be used to evaluate whether the analysis of brain electroencephalographic signals could track early progression from MCI to mild AD via large population screening. There is growing interest in this technique because of its low cost, widespread availability, and noninvasiveness. This paper aimed to determine whether a specific analysis of EEG rhythms, exploring brain SW characteristics, could predict—when combined with a genetic risk evaluation gleaned from the ApoE genotype—the risk of conversion from MCI to AD as a first-level screening method with appropriate specificity/sensitivity. This type of combined approach (ie, graph theory for EEG signals and ApoE genotyping) has been previously utilized with diagnostic purposes to distinguish between healthy elderly and AD subjects[31,32]; however, to the best of our knowledge, such an approach has never been previously reported for prognostic purposes, namely to discriminate prodromal-to-AD from nonprodromal in a sample of MCI subjects.

Healthy brain organization reflects an optimal balance of functional integration and segregation; such a scenario is termed SW. SW characteristics reflect complex inhibitory and excitatory brain circuits consisting of functionally specialized regions that continuously and mutually cooperate to acquire, share, and integrate information in a constant state of dynamic fluctuations that is also governed by a number of variables—including attention, emotion, motivation, and arousal—influencing network performance. Connections between neuronal assemblies reflect segregation and integration processes, as revealed by local clustering (segregation) and path length (integration).

Here, a statistically significant difference in the SW organization of converted subjects (particularly among rapid—i.e. within 1–2 years—converters) was found, and the SW distributions in the EEG frequency bands of interest corresponded to aMCI-S; however, it was also shown that aMCI-C subjects do have SW characteristics very similar to those of AD patients 1 to 2 years before conversion (time 0 of the study).

Many studies have looked at topological changes in the brain networks with different modalities and have examined the structural and diffusion tensor imaging MRI, EEG/magnetoencephalography, and functional MRI reviewed by Xie and He.[52] Therefore, AD is more often considered a disconnection syndrome,[49] and brain topology can be represented by a progressive derangement of the brain organization in hub regions and long-range connections causing SW architecture alteration. Due to decreasing local and global connectivity parameters, the large-scale functional brain network organization in AD deviates from the optimal SW architecture toward a more "ordered" type (as reflected by lower SW values), leading to less efficient information exchange across brain areas that is in line with the disconnection hypothesis of AD.[49]

Here, an abnormal increase in graph theory parameters in converted subjects, with respect to aMCI-S, has been observed for the low alpha rhythm, along with a decrease in the delta and gamma rhythms. Such an effect should be interpreted in light of the physiological role that the alpha rhythm plays. Alpha frequencies constitute the leading characteristic of normal EEG activity at waking rest, usually defined as the "idling rhythms" of the adult brain.[53] Several studies support the hypothesis that alpha is a deterministic chaotic signal with several functional correlates ranging from memory formation to sensory-motor processing.[54] In healthy individuals, alpha rhythm works as an oscillatory component of brain activity and can therefore be interpreted as a basic form of information transmission in the brain.[55] Moreover, event-related activity studies have shown a positive correlation between alpha frequency and the speed of information processing, as well as a good cognitive performance.[55]

For the delta band, it is argued that, in a waking state, such EEG rhythms are poorly represented, thus reflecting a condition of likely alpha-delta "reciprocal inhibition."[11] Furthermore, it is well known that the anatomical or functional disconnection of lesioned cortical areas generates spontaneous slow oscillations in the delta range

in virtually all recorded neurons. The SW decrease in the delta band represents a type of structured behavior that could be interpreted as an increase in delta activity and a functional inhibition. The opposite holds true for the alpha band.

A SW decrease in the gamma band in the converted MCI subjects is in line with previous evidence[26] showing a decrease of the SW gamma band in AD patients with respect to MCI and control subjects. The gamma band (>30Hz) includes high-frequency EEG oscillations that mediate information transfer between cortical and hippocampal structures for memory processes,[56] particularly through feed-forward mechanisms[57] and coherent phase-coupling between oscillations from different structures.[58] Both animal and human studies provide evidence that gamma oscillations play a fundamental role in memory tasks. Gamma neural activity is involved in numerous cognitive functions—including visual object processing, attention, and memory[59]—and is also strongly associated with behavioral performance (accuracy and reaction time) in several memory tasks, including tasks probing episodic memory, encoding, and retrieval.[60] Furthermore, microelectrode intraneural recordings have demonstrated that gamma oscillations are pivotal in spike phase synchronization, which is at the base of EEG connectivity mechanisms.[61]

The ROC curve for EEG SW characteristics showed a >60% sensitivity (AUC = 0.64, indicating moderate classification accuracy) for classifying the MCI state as a prodromal indicator of AD when all subjects were used. The present findings are in line with those of previous studies[26,39,62] in which SW characteristics were found to have decreased in patients with AD with respect to MCI in low-frequency EEG rhythms. In other words, the MCI connectivity pattern was less random than that of the AD group. Moreover, significant differences between healthy elderly MCI subjects and AD patients have been demonstrated by showing that physiological brain aging presents greater specialization (although lower values) of SW EEG rhythm characteristics that are higher than normal in slow frequencies and lower in alpha bands.[28] Finally, the control analysis, with respect to AD patients, showed that aMCI-C presented a graph theory pattern that was practically identical to that of AD. These findings suggest that EEG connectivity analysis, combined with neuropsychological evaluation in MCI, could be of great help in early identification of this condition as a first-line screening method and a means to intercept those subjects with a high risk for rapid progression to AD.

ROC curves showed that, when both phenotype and genotype characteristics (obtained at a low cost with widely available ApoE technology) were combined, the accuracy remarkably increased to 91.78% (AUC = 0.97, indicating an optimal classification accuracy) for classifying the MCI state as prodromal of AD. This result is in line with the finding that the ε4 allele of the *APOE* gene is a major genetic risk factor for pathogenesis of late onset AD[33,34]; it also suggests that SW characteristics and ApoE contribute to predict outcome in a synergistic way with little overlap. We also verified that the EEG SW measures played a particularly relevant role in *APOE* e4 noncarriers. Of note, a more homogenous population showed decreased accuracy, but it should be also noted that the more homogenous population consisted of a lower number of subjects.

Altogether, our findings clearly demonstrate that ApoE genotype and EEG connectivity reflect different types of "aggressors" responsible for neurodegenerative mechanisms and that they nicely integrate each other when considered in combination.

Is the graph theoretical model superior to other types of EEG analysis in an AD diagnostic context? To answer this question, we compared the same type of classifier to other methods of EEG analysis currently used for AD studies; we then applied the results to the same EEG epochs utilized for graph valuation, namely spectral coherence and power spectrum, still in combination with ApoE genotyping. The analysis showed 51.79% sensitivity, 100% specificity, and 68.86% accuracy. These results are promising but less significant than those from our SW analysis.

The intrinsic characteristics of EEG rhythms contain relevant information on neurodegenerative processes underlying AD. These processes begin long before clinical symptoms manifest, by deranging the synaptic transmissions and the efficacy of brain dynamic connections.[49] A plastic reorganization of the surviving neuronal circuitries—the neural "reserve"—affects daily living abilities. This is due to prolonged neurodegeneration toward a network maintenance of functional connections.[11,49,63] In aMCI-C subjects, the SW characteristics provided reliable predictions of aMCI to AD progression within a relatively short time frame. Moreover, rapid progression from aMCI to AD heralds an aggressive type of dementia with a rapid degradation of daily life skills.

In conclusion, EEG connectivity analysis, combined with a neuropsychological MCI pattern and ApoE genotyping, could represent a combination of biomarkers that are of great help in the early identification of MCI prodromal to AD. This combination represents a multimodal, low-cost, and noninvasive approach, one that utilizes widely available techniques that, when combined, reach high sensitivity/specificity and good classification accuracy on an individual basis (>0.97 of AUC). It could therefore

be used to effectively determine the risk of the progression to AD in MCI patients and should be considered a first line of screening.

Acknowledgment

This work was supported by the Italian Ministry of Health [RicercaCorrente]; the "NEUROMASTER: NEUROnavigatedMAgneticSTimulation in patients with mild-moderate Alzheimer's disease, combined with Effective cognitive Rehabilitation" (grant GR-2013-02358430).

Author Contributions

P.M.R., F.V., and F.M.: study concept and design; G.L., V.G., F.D.T., P.P., F.V., F.M., F.I., and C.M.: data acquisition and analysis including statistical evaluation; F.V., F.M., and P.M.R.: drafting the manuscript and figures.

Potential Conflicts of Interest

Nothing to report.

References

1. Petersen RC, Smith GE, Ivnik RJ, et al. Apolipoprotein E status as a predictor of the development of Alzheimer's disease in memory-impaired individuals. JAMA 1995;273:1274–1278.
2. Petersen RC, Doody R, Kurz A, et al. Current concepts in mild cognitive impairment. Arch Neurol 2001;58:1985–1992.
3. Scheltens P, Fox N, Barkhof F, De CC. Structural magnetic resonance imaging in the practical assessment of dementia: beyond exclusion. Lancet Neurol 2002;1:13–21.
4. Petersen RC. Mild cognitive impairment as a diagnostic entity. J Intern Med 2004;256:183–194.
5. Petersen RC, Lopez O, Armstrong MJ, et al. Practice guideline update summary: Mild cognitive impairment: Report of the Guideline Development, Dissemination, and Implementation Subcommittee of the American Academy of Neurology. Neurology 2018;90:126–135.
6. Nathan PJ, Lim YY, Abbott R, et al. Association between CSF biomarkers, hippocampal volume and cognitive function in patients with amnestic mild cognitive impairment (MCI). Neurobiol Aging 2017; 53:1–10.
7. Roberts R, Knopman DS. Classification and epidemiology of MCI. Clin Geriatr Med 2013;29:753–772.
8. Getsios D, Blume S, Ishak KJ, et al. An economic evaluation of early assessment for Alzheimer's disease in the United Kingdom. Alzheimers Dement 2012;8:22–30.
9. Wimo A, Jonsson L, Bond J, et al. The worldwide economic impact of dementia 2010. Alzheimers Dement 2013;9:1–11.
10. Vecchio F, Babiloni C, Lizio R, et al. Resting state cortical EEG rhythms in Alzheimer's disease: toward EEG markers for clinical applications: a review. Suppl Clin Neurophysiol 2013;62:223–236.
11. Rossini PM, Del Percio C, Pasqualetti P, et al. Conversion from mild cognitive impairment to Alzheimer's disease is predicted by sources and coherence of brain electroencephalography rhythms. Neuroscience 2006;143:793–803.
12. Huang C, Wahlund L, Dierks T, et al. Discrimination of Alzheimer's disease and mild cognitive impairment by equivalent EEG sources: a cross-sectional and longitudinal study. Clin Neurophysiol 2000;111: 1961–1967.
13. Koenig T, Prichep L, Dierks T, et al. Decreased EEG synchronization in Alzheimer's disease and mild cognitive impairment. Neurobiol Aging 2005;26:165–171.
14. Jelic V, Johansson SE, Almkvist O, et al. Quantitative electroencephalography in mild cognitive impairment: longitudinal changes and possible prediction of Alzheimer's disease. Neurobiol Aging 2000; 21:533–540.
15. Adler G, Brassen S, Jajcevic A. EEG coherence in Alzheimer's dementia. J Neural Transm (Vienna) 2003;110:1051–1058.
16. Prichep LS, John ER, Ferris SH, et al. Prediction of longitudinal cognitive decline in normal elderly with subjective complaints using electrophysiological imaging. Neurobiol Aging 2006;27:471–481.
17. de Haan W, Mott K, van Straaten EC, et al. Activity dependent degeneration explains hub vulnerability in Alzheimer's disease. PLoS Comput Biol 2012;8:e1002582.
18. Dauwels J, Vialatte F, Cichocki A. Diagnosis of Alzheimer's disease from EEG signals: where are we standing? Curr Alzheimer Res 2010; 7:487–505.
19. Babiloni C, Vecchio F, Lizio R, et al. Resting state cortical rhythms in mild cognitive impairment and Alzheimer's disease: electroencephalographic evidence. J Alzheimers Dis 2011;26(suppl 3):201–214.
20. Vecchio F, Miraglia F, Quaranta D, et al. Cortical connectivity and memory performance in cognitive decline: a study via graph theory from EEG data. Neuroscience 2016;316:143–150.
21. Vecchio F, Miraglia F, Piludu F, et al. "Small world" architecture in brain connectivity and hippocampal volume in Alzheimer's disease: a study via graph theory from EEG data. Brain Imaging Behav 2017; 11:473–485.
22. Dauwels J, Vialatte F, Musha T, Cichocki A. A comparative study of synchrony measures for the early diagnosis of Alzheimer's disease based on EEG. Neuroimage 2010;49:668–693.
23. Friston KJ. Functional and effective connectivity in neuroimaging: a synthesis. Human Brain Mapp 1994;2:56–78.
24. Watts DJ, Strogatz SH. Collective dynamics of 'small-world' networks. Nature 1998;393:440–442.
25. Bassett DS, Bullmore E. Small-world brain networks. Neuroscientist 2006;12:512–523.
26. Vecchio F, Miraglia F, Marra C, et al. Human brain networks in cognitive decline: a graph theoretical analysis of cortical connectivity from EEG data. J Alzheimers Dis 2014;41:113–127.
27. Vecchio F, Miraglia F, Bramanti P, Rossini PM. Human brain networks in physiological aging: a graph theoretical analysis of cortical connectivity from EEG data. J Alzheimers Dis 2014;41:1239–1249.
28. Vecchio F, Miraglia F, Curcio G, et al. Cortical brain connectivity evaluated by graph theory in dementia: a correlation study between functional and structural data. J Alzheimers Dis 2015;45:745–756.
29. Stam CJ, Jones BF, Nolte G, et al. Small-world networks and functional connectivity in Alzheimer's disease. Cereb Cortex 2007;17: 92–99.
30. de Haan W, Pijnenburg YA, Strijers RL, et al. Functional neural network analysis in frontotemporal dementia and Alzheimer's disease using EEG and graph theory. BMC Neurosci 2009;10:101.
31. Kramer G, van der Flier WM, de Langen C, et al. EEG functional connectivity and ApoE genotype in Alzheimer's disease and controls. Clin Neurophysiol 2008;119:2727–2732.
32. Canuet L, Tellado I, Couceiro V, et al. Resting-state network disruption and APOE genotype in Alzheimer's disease: a lagged functional connectivity study. PLoS One 2012;7:e46289.
33. Huang Y, Mucke L. Alzheimer mechanisms and therapeutic strategies. Cell 2012;148:1204–1222.

34. Giri M, Zhang M, Lu Y. Genes associated with Alzheimer's disease: an overview and current status. Clin Interv Aging 2016;11:665–681.
35. Winblad B, Palmer K, Kivipelto M, et al. Mild cognitive impairment—beyond controversies, towards a consensus: report of the International Working Group on Mild Cognitive Impairment. J Intern Med 2004;256:240–246.
36. McKhann GM, Knopman DS, Chertkow H, et al. The diagnosis of dementia due to Alzheimer's disease: recommendations from the National Institute on Aging-Alzheimer's Association workgroups on diagnostic guidelines for Alzheimer's disease. Alzheimers Dement 2011;7:263–269.
37. Petersen RC, Smith GE, Waring SC, et al. Aging, memory, and mild cognitive impairment. Int Psychogeriatr 1997;9(suppl 1):65–69.
38. Portet F, Ousset PJ, Visser PJ, et al. Mild cognitive impairment (MCI) in medical practice: a critical review of the concept and new diagnostic procedure. Report of the MCI Working Group of the European Consortium on Alzheimer's Disease. J Neurol Neurosurg Psychiatry 2006;77:714–718.
39. Miraglia F, Vecchio F, Bramanti P, Rossini PM. EEG characteristics in "eyes-open" versus "eyes-closed" conditions: small-world network architecture in healthy aging and age-related brain degeneration. Clin Neurophysiol 2016;127:1261–1268.
40. Miraglia F, Vecchio F, Rossini PM. Searching for signs of aging and dementia in EEG through network analysis. Behav Brain Res 2017; 317:292–300.
41. Pascual-Marqui RD. Standardized low-resolution brain electromagnetic tomography (sLORETA): technical details. Methods Find Exp Clin Pharmacol 2002;24(suppl D):5–12.
42. Pascual-Marqui RD. Instantaneous and lagged measurements of linear and nonlinear dependence between groups of multivariate time series: frequency decomposition. arXiv 2007. Available at: https://arxiv.org/ftp/arxiv/papers/0711/0711.1455.pdf
43. Rubinov M, Sporns O. Complex network measures of brain connectivity: uses and interpretations. Neuroimage 2010;52:1059–1069.
44. Hixson JE, Vernier DT. Restriction isotyping of human apolipoprotein E by gene amplification and cleavage with HhaI. J Lipid Res 1990; 31:545–548.
45. Lehmann D, Faber PL, Tei S, et al. Reduced functional connectivity between cortical sources in five meditation traditions detected with lagged coherence using EEG tomography. Neuroimage 2012;60: 1574–1586.
46. Barnett JH, Lewis L, Blackwell AD, Taylor M. Early intervention in Alzheimer's disease: a health economic study of the effects of diagnostic timing. BMC Neurol 2014;14:101.
47. Wimo A, Guerchet M, Ali GC, et al. The worldwide costs of dementia 2015 and comparisons with 2010. Alzheimers Dement 2017;13:1–7.
48. Teipel SJ, Kurth J, Krause B, Grothe MJ. The relative importance of imaging markers for the prediction of Alzheimer's disease dementia in mild cognitive impairment—beyond classical regression. Neuroimage Clin 2015;8:583–593.
49. D'Amelio M, Rossini PM. Brain excitability and connectivity of neuronal assemblies in Alzheimer's disease: from animal models to human findings. Prog Neurobiol 2012;99:42–60.
50. Petersen RC, Thomas RG, Aisen PS, et al. Randomized controlled trials in mild cognitive impairment: sources of variability. Neurology 2017;88:1751–1758.
51. Sachdev PS, Lipnicki DM, Kochan NA, et al. The prevalence of mild cognitive impairment in diverse geographical and ethnocultural regions: the COSMIC collaboration. PLoS One 2015;10:e0142388.
52. Xie T, He Y. Mapping the Alzheimer's brain with connectomics. Front Psychiatry 2011;2:77.
53. Niedermeyer E, da Silva FL. *Electroencephalography: basic principles, clinical applications, and related fields*. Philadelphia, PA: Lippincott Williams & Wilkin, 2005.
54. Schurmann M, Basar E. Functional aspects of alpha oscillations in the EEG. Int J Psychophysiol 2001;39:151–158.
55. Klimesch W. EEG alpha and theta oscillations reflect cognitive and memory performance: a review and analysis. Brain Res Brain Res Rev 1999;29:169–195.
56. Vinck M, Womelsdorf T, Buffalo EA, et al. Attentional modulation of cell-class-specific gamma-band synchronization in awake monkey area v4. Neuron 2013;80:1077–1089.
57. Abeles M. *Corticonics: neural circuits of the cerebral cortex*. New York, NY: Cambridge University Press, 1991.
58. Fries P. A mechanism for cognitive dynamics: neuronal communication through neuronal coherence. Trends Cogn Sci 2005;9:474–480.
59. Tallon-Baudry C, Bertrand O, Peronnet F, Pernier J. Induced gamma-band activity during the delay of a visual short-term memory task in humans. J Neurosci 1998;18:4244–4254.
60. Kaiser J, Heidegger T, Lutzenberger W. Behavioral relevance of gamma-band activity for short-term memory-based auditory decision-making. Eur J Neurosci 2008;27:3322–3328.
61. Nikolic D, Fries P, Singer W. Gamma oscillations: precise temporal coordination without a metronome. Trends Cogn Sci 2013;17:54–55.
62. de Haan W, van der Flier WM, Koene T, et al. Disrupted modular brain dynamics reflect cognitive dysfunction in Alzheimer's disease. Neuroimage 2012;59:3085–3093.
63. Ferreri F, Pauri F, Pasqualetti P, et al. Motor cortex excitability in Alzheimer's disease: a transcranial magnetic stimulation study. Ann Neurol 2003;53:102–108.